Extended Dipolar Chain Model for Ion Channels: Electrostriction Effects and the Translocational Energy Barrier

Miguel Sancho,*‡ Michael B. Partenskii,* Vladimir Dorman,§ and Peter C. Jordan*

*Department of Chemistry, Brandeis University, Waltham, Massachusetts 02254 USA; ‡Departamento de Fisica Aplicada III, Universidad Complutense de Madrid, 28040 Madrid, Spain; and §Rampage Systems, Inc., Waltham, Massachusetts 02154 USA

ABSTRACT We reinvestigate the dipolar chain model for an ion channel. Our goal is to account for the influence that ion-induced electrostriction of channel water has on the translocational energy barriers experienced by different ions in the channel. For this purpose, we refine our former model by relaxing the positional constraint on the ion and the water dipoles and by including Lennard-Jones contributions in addition to the electrostatic interactions. The positions of the ion and the waters are established by minimization of the free energy. As before, interaction with the external medium is described via the image forces. Application to alkali cations show that the short range interactions modulate the free energy profiles leading to a selectivity sequence for translocation. We study the influence of some structural parameters on this sequence and compare our theoretical predictions with observed results for gramicidin.

INTRODUCTION

Ion channels, to be specific, are believed to have a narrow region that acts as a selectivity filter (Hille, 1992). Although not mandatory, many channel models presume that there is an abutting region in which the concerted ion-water movement is single file. Direct experimental evidence determining the length of such single files is scant. For the model system gramicidin, this distance has been determined with reasonable accuracy by an amalgam of theoretical and experimental methods to be ~20–25 Å (for review, see Wallace, 1990). Inferences with respect to physiological systems indicate that a single file may be as short as 7–10 Å in a high conductance K-channel (Miller, 1982) and long enough to permit multiple occupancy (conceivably as long as 50 Å), i.e., the delayed and inward rectifying K-channels (Hille and Schwartz, 1978). In such single-file regions, the ion must have shed all but two of its waters of solvation and be stabilized by interaction with charged and polar groups of the channel peptide. In addition, its immediate electrical environment is vastly different from bulk water since the peptide, with which it is in intimate contact, is far less orientationally polarizable than water. The ion and the channel water molecules are surrounded by a domain of low to intermediate dielectric constant. Because water in narrow channels cannot form the extended hydrogen-bonded networks characteristic of liquid water, this region quite probably behaves very differently from bulk water. There are suggestions that channel water forms a distinctly different phase (Chiu et al., 1993). Because the energy barriers for ion permeation must be low (turnover is $\sim 10^7\ s^{-1}$), it has often been presumed that the channel forms an electrically permittive pathway (Levitt, 1978; Jordan, 1984; Jordan et al., 1989; Sancho and Martinez, 1991; Monoi, 1991). To better characterize this physiologically significant region, we have developed an exactly soluble model describing critical features of the single file. The channel is modeled as a linear chain comprising the ion and a limited number of water molecules (Partenskii et al., 1991a). This array is embedded in a continuum dielectric slab that accounts, in approximate fashion, for the influence of the surrounding protein. The whole ensemble is sandwiched between continuum dielectrics descriptive of bulk water. In this way we have been able to formulate exact solutions to the associated statistical mechanical problem.

In our previous studies of this model, we found that water in the channel can be strongly polarized by the field of an ion; it cannot readily reorient under an applied field, so that with an ion in the channel, water's effective orientational susceptibility drops precipitously (Partenskii et al., 1991a; Partenskii and Jordan, 1992a, b). This view differs from the familiar continuum models that describe a channel as a high permittivity and, consequently, low image energy pathway for the ion along the pore (Levitt, 1978; Jordan, 1984; Jordan et al., 1989; Sancho and Martinez, 1991; Monoi, 1991; Martinez et al., 1992). The associated electrostatic free energy barriers are invariably too high to be consistent with observed permeation rates; the effective dielectric constant for channel water, with an ion present, is certainly less that 10, and possibly as low as 4–5 (Partenskii and Jordan, 1992a). If we consider molecular dynamics (MD) simulations in seeking the origin of the required free energy barrier reduction, we note that the properties of water near a charged particle, whether in a gas phase cluster, inside a narrow channel or in the bulk medium can be significantly altered with respect to those of water molecules not involved in ionic solvation (Sung and Jordan, 1986; Lin and Jordan, 1989; Jordan, 1990; Duca and Jordan, 1993). In an occupied ion channel, mean water-water correlations can be strongly ion-dependent and both ion-water and water-water correlations in this environment can be very different from those in bulk

Received for publication 13 September 1994 and in final form 7 November 1994.

Address reprint requests to Dr. Peter C. Jordan, Department of Chemistry, Brandeis University, Waltham, MA 02254-9110. Tel.: 617-736-2540; Fax: 617-736-2516; E-mail: jordan@binah.cc.brandeis.edu

0006-3495/95/02/427/07 $2.00

water. The contribution of electrostriction is known to be ion-specific and to affect the ion's solvation free energy (Jayaram et al., 1989); thus, it modifies free energy profiles in an ion-dependent fashion. In this study we further explore the relationship between the microscopic description of a narrow ion pore and macroscopic electrostatic models, by incorporating an additional microscopic feature into the calculation. To this end we relax the restriction of rigid spheres in our chain model and allow the ion and the water molecules to interact under the combined influence of electrostatic and short range interactions. We show that the energy lowering due to this relaxation is not enough to account for the observed permeation rates; other contributions are required, probably those arising from specific consideration of the protein (or peptide) charge distribution and from short range differential solvation interactions as the ion is partially dehydrated upon entering a pore and specifically bound to polar groups lining a channel. At the same time we address the important question of selectivity and find that the modulation of the energy barriers due to electrostriction is consistent with the observed translocational selectivity sequence in gramicidin channels. Finally, we note that electrostriction, as gauged by ion-water and water-water separations, varies significantly as ions translocate through a pore.

MODEL AND BASIC EQUATIONS

The model presented previously (Partenskii et al., 1991a; Partenskii and Jordan, 1992a, b) consists of a single-file chain of an ion and a fixed number of water molecules embedded in a dielectric slab of uniform permittivity $\epsilon_{background}$, illustrated in Fig. 1 for the specific case of seven waters. The slab is surrounded on both sides by uniform continuum solvent of high dielectric constant. The number of particles in the single file is chosen to be representative of gramicidin, where both MD studies and electrokinetic experiments indicate that 7 to 9 water molecules accompany ions moving through a gramicidin channel (Levitt, 1984; Mackay et al., 1984; Skerra and Brickmann, 1987; Jordan, 1990; Roux and Karplus, 1991a, b; Hille, 1992). In this approach water is modeled by a sphere with a reorientable point dipole (μ = 1.86 Debye) at its center; the ion is described as a sphere with a point charge at its center. Because the problem is one-dimensional and cylindrical symmetry is imposed, exact solutions of the statistical mechanical problem, including all long range interactions with the surrounding solvent, have been formulated (Partenskii et al., 1991a; Partenskii and Jordan, 1992a). The model can thus describe major features accounting for orientational ordering in real channel systems at finite temperatures. However, high frequency ion-water and water-water processes, because of electronic polarizability, interparticle collisions, off-axis motions, dipole moment fluctuations (due, e.g., to bond bending) are not treated in this picture. It also makes no attempt to describe the detailed interaction of either ion or waters with molecular charge distribution of the channel forming peptide.

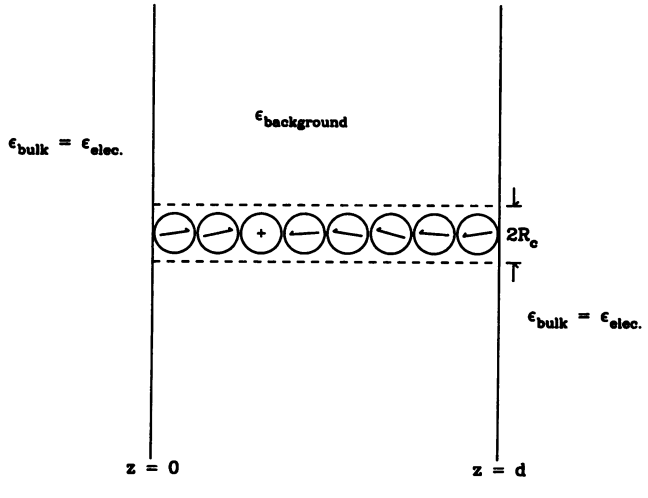

FIGURE 1 Semi-discrete model of the dielectric geometry of a water-lipid-channel ensemble. The channel radius is R_c, and the lipid-bulk water boundaries are the planes $z = 0$ and $z = d$. Water (point dipoles embedded in a sphere) and an ion (point charge embedded in a sphere) for a linear chain. The chain length is variable, reflecting the influence of ionic size and the background dielectric (see text). $\epsilon_{background}$ is chosen to approximate the permittivity of the channel forming peptide and the high frequency dielectric behavior of water (see text).

This model replicates important features of real ion channel systems. There is a linear single-file region containing an ion and a limited number of waters; this molecular column is surrounded by a continuum dielectric representative of both peptide and lipid. The whole ensemble is sandwiched between dielectric continua of $\epsilon = 80$, representative of bulk water. The connection to gramicidin, which has an unusually long single-file region, is made quite simply, by focusing on a molecular column of an ion and seven waters.

Assigning a permittivity value of $\epsilon_{background} = 2$ accounts for both the dielectric properties of the membrane (Dilger et al., 1982; Fettiplace et al., 1971) and the influence of the electronic polarizability of the water inside the pore, the latter estimated from the optical refractive index. However, the proper assignment of a high frequency ϵ for water in this approach is far from certain. The statistical mechanical problem of the dipoles' orientational correlation is treated exactly; for water these are processes on the 10–100 GHz time scale (Franks, 1973). Faster motions, due to interparticle collisions, are not considered. The dipoles are thus in an electrical environment with an ϵ that accounts for processes rapid compared to rotational relaxation, i.e., >100 GHz. At ultrahigh frequency (>100 THz) water's ϵ is 2 and, as already noted, it is determined by the electronic polarization (the optical refractive index). However, from the behavior of bulk water, there is clearly an intermediate domain, faster than rotational relaxation but slower than electronic relaxation, in which $\epsilon \approx 4$ (Franks, 1973; Hasted, 1973). In the model, electronic polarization and these Newtonian high frequency relaxation processes are accounted for by assigning an ϵ of 4 to the immediate electrical environment of the ion-dipole chain. Then $\epsilon_{background}$ would decrease from 4 to 2 in moving radially outward from the channel axis. Consequently, we

consider values of $\epsilon_{background}$ between 2 and 4 and, for simplicity of computation, take $\epsilon_{background}$ to be constant. This latter assumption makes little difference because the computation is dominated by the value of ϵ in the immediate vicinity of the channel (<7 Å from the axis) (Partenskii and Jordan, 1992b). For modeling gramicidin, the peptide, with its moderately high electrical permittivity (Tredgold and Hole, 1976; Monoi, 1991; Hille, 1992), has a radius of ≈10 Å (Koeppe and Kimura, 1984; Mackay et al., 1984); thus, the membrane is too far away to influence properties in the channel for the model being studied.

The orientational polarization of water is treated by placing point dipoles with a dipole moment determined from a calculation that ignores the Lennard-Jones forces at the center of each spherical water molecule. The permittivity of the external medium, which is much greater than that of the membrane, is approximated as $\epsilon_{elec.} = \infty$; this introduces no serious error (Partenskii and Jordan, 1992a, b) and is exact in the limit of high ionic strength (our unpublished results). It is thus possible to account simply for long-range electrostatic interaction, using the method of images. Effects due to the more polarizable channel-forming peptide as well as that of ion-induced charge reorganization (in a gramicidin-like model, reorientation of carbonyl groups at the peptide-pore interface), have been analyzed elsewhere (Partenskii et al., 1991a; Partenskii and Jordan, 1992b) and are not explicitly considered here. Our system Hamiltonian is

$$H = W_{dd} + W_{Ion} + W_{LJ} + W_{Born}, \qquad (1)$$

where W_{dd} is the dipole-dipole interaction energy (including the image dipole contributions), W_{Ion} is the interaction energy of the ion with its own image and with the dipoles and their images, W_{Born} is the energy required to transfer the ion from bulk, where $\epsilon = 80$, to the channel interior where $\epsilon = \epsilon_{background}$ (between 2 and 4). These three contributions have been discussed previously (Partenskii et al., 1991a, b; Partenskii and Jordan, 1992b). The additional term, W_{LJ}, describing the Lennard-Jones interaction between particles has the form

$$W_{LJ} = \sum_{\epsilon I\text{-}W} [(\sigma_{I\text{-}W}/r_k)^{12} - (\sigma_{I\text{-}W}/r_k)^6] + \sum\sum_{\epsilon W\text{-}W} [(\sigma_{W\text{-}W}/r_{ij})^{12} - (\sigma_{W\text{-}W}/r_{ij})^6] + W_L + W_R, \qquad (2)$$

where W_L and W_R represent two additional short range terms that account for interaction of the first and last particle in the chain with the respective left and right pore-bulk medium interface. For these terms we also choose a 6–12 potential approximation where the distances are those between the particles and their first images; the interaction parameters are those corresponding to the ion-water or water-water potential depending on what particle is in the first or last position. To determine the Lennard-Jones parameters, we average the values for the corresponding isoelectronic noble gas atoms (Hirschfelder et al., 1954) with those for TIP4P water (Jorgensen et al., 1983) using standard combination rules (Kong, 1973); the results are listed in Table 1.

TABLE 1 Lennard-Jones parameters for ion-water and water-water interaction

Interacting particles	σ (Å)	ϵ (kJ/mol)
Li^+-Water	2.89	0.180
Na^+-Water	2.96	0.434
K^+-Water	3.28	0.812
Cs^+-Water	3.54	1.083
Water-Water	3.16	0.649

To obtain equilibrium distances and the corresponding total internal energies, we make an initial guess as to the positions of both ion and waters and compute the waters' mean dipole moment vectors and the corresponding pair correlation functions, $\langle p_i \rangle$ and $\langle p_i \cdot p_j \rangle$, using the method developed previously (Partenskii et al., 1991a) extended to account fully for dipolar correlation (our earlier studies focussed exclusively on the averages $\langle p_i \rangle$, a mean field approximation reliable as long as $\epsilon_{background}$ is small). Using the values for $\langle p_i \rangle$ and $\langle p_i \cdot p_j \rangle$, we permit the ion-water and water-water separations to relax, thus achieving a balance between attractive (electrostatic, van der Waals) and repulsive (hard core) interactions. The correlation functions decompose into axial and normal components, of which only the axial part noticeably affects the free energy. The new equilibrium state is determined by minimizing the free energy G (Partenskii et al., 1991a) determined from the Hamiltonian, Eq. 1, with respect to the eight positions z_i with $1 \le i \le 8$. At each step we take the length of the channel, necessary to calculate the position of images, as $h = z8 + (z8 - z7)/2$; thus, the channel is slightly extendible. With the functions $\langle p_i \rangle$ and $\langle p_i \cdot p_j \rangle$ in hand, we determine a new set of equilibrium positions using a numerical procedure based on a downhill simplex method (Press, 1992) for the free energy minimization. We then recompute dipole moments and dipolar correlation functions based on the new set of ion and dipole locations, and continue the process until self-consistency is attained. With a reasonable initial guess, convergence requires no more than two iterations.

To recapitulate, there are three distinct contributions to the model Hamiltonian: the Born energy for transferring an ion from the electrolyte to the dipolar chain; the full ion-dipole and dipole-dipole interaction, including all image interactions with the electrolyte; and the Lennard-Jones interaction between the various groups in the chain. The ion and dipoles lie on a line; both dipolar orientations and interparticle spacings are variable. Because of thermal interaction, both orientations and spacings should fluctuate about their equilibrium values. Our solution accounts for both orientational and separational variability, and for thermally driven orientational fluctuations. What we do not account for is the thermal coupling of translational fluctuation with orientational fluctuation. Our computational method fixes interparticle separations, then lets the dipoles re-equilibrate (thermally). With new dipolar directions fixed, we determine the minimum in the interaction energy and establish a new set of interparticle separations. These form the basis for the next thermal equilibration of the dipolar orientations. Qualitatively, there is a clear inverse correlation between dipolar alignment and in-

terparticle separation. Our procedure for computing ionic location accounts for this, although the positions we determine are just approximate, because instantaneous, fluctuationally driven, orientational-positional correlation is not handled by our method of solution. Ion-dependent electrostriction has its greatest influence on the behavior of the ion's first and second neighbor waters for which water is strongly oriented and the separational fluctuations small. Interaction with remote water dipoles, where separational fluctuations are more important, contributes little to the ion-dependent free energy differences. Thus, we can expect that neglecting the instantaneous, fluctuationally driven component of the orientation-position correlations has little influence on the energetics.

RESULTS AND DISCUSSION

The total transfer energy from water to the channel for alkali ions at sites 1 and 4 along the channel axis are given in Table 2 for the two limiting cases, $\epsilon_{background} = 2$ and 4. The energies are relative to the ion in aqueous solution and include the Born energy with ionic radius in the channel defined as $(d_{I\text{-}W} - 0.5 \cdot d_{W\text{-}W})$ with d either the ion-water or the water-water distance, respectively. We have assumed that ionic radii do not change in the process of channel solvation; even if the ionic radii in bulk water differed by as much as 25% from their values in the pore, the associated energy difference would be relatively insignificant, <2.5 kJ mol^{-1}. In establishing these data, the ion and the waters have adjusted their separations to minimize the total energy of the ensemble. Assuming permeation is diffusive in nature (Jakobsson and Chiu, 1987), using the Nernst-Planck expression for ionic flux in the ohmic domain (Levitt, 1986), we can use our transfer energies to obtain very rough estimates of channel conductance. For 0.01 M electrolyte, for which the single-channel conductance is ~1 pS, we obtain ridiculously small values, between 10^{-11} and 10^{-6} pS for Cs^+ and between 10^{-43} and 10^{-21} pS for Li^+, as $\epsilon_{background}$ increases from 2 to 4. As is clear from these data and as we have demonstrated (Partenskii and Jordan, 1992b) previously, for plausible values of $\epsilon_{background}$ the transfer energy between water and a structureless pore with gramicidin-like dimensions is substantially larger than any reasonable estimate of the permeation free energy barrier.

There are three obvious possible reasons for this limitation. This model may exaggerate ionic stabilization in bulk water. It does not specifically include electrostatic interaction between both ion and waters and the peptide charge distribution. It also ignores the influence of short range differential solvation interactions as the ion is partially dehydrated upon entering a pore and specifically bound to polar groups lining a channel. We have already shown that the mesoscopic influence of the peptide, although stabilizing, does not reduce transfer energies sufficiently to be consistent with observed permeation rates (Partenskii and Jordan, 1992b, 1993). Thus, short range differential solvation, which can only be treated by means of a molecular theory, must significantly influence permeation.

TABLE 2 Total free energy of transfer, ΔG_{tot}, (kJ/mol) for alkali cations at two channel sites for $\epsilon_{background} = 2$ and 4

Ion	Site #	ΔG_{tot} ($\epsilon = 2$)	ΔG_{tot} ($\epsilon = 4$)
Li^+	1	196.5	97.5
	4	247.9	122.6
Na^+	1	117.6	61.4
	4	166.5	85.5
K^+	1	50.5	30.1
	4	95.3	52.5
Cs^+	1	23.1	17.9
	4	65.7	39.1

Because of gramicidin's quasi-periodicity, it is reasonable to believe that ion-specific changes in differential solvation interactions do not vary greatly as the ion translocates through the channel (i.e., the difference in binding energy between Na^+ and Cs^+ is only weakly site-dependent). Thus, we focus on the translocation energies, defined as the energy associated with moving from the binding site near the channel mouth across the electrostatic barrier near the channel center. Fig. 2 depicts the free energy profiles for monovalent cations in a channel with seven water molecules (an eight-source model) as functions of $\epsilon_{background}$. The translocation barrier is *defined* as the energy difference associated with moving the ion from position 1 (the mouth) to position 4 (the midpoint). The absolute energies are of no significance. Each set of profiles has been adjusted so that energies are *relative* to that of an ion at the first site inside the channel mouth. As $\epsilon_{background}$ increases, ion-induced long-range orientational correlation of the water molecules is substantially reduced (Partenskii and Jordan, 1992b). One consequence is that energy differences between successive ion sites decreases monotonically. There is another obvious systematic trend; regardless of $\epsilon_{background}$, the translocational barriers decrease as ionic size increases, precisely reproducing Eisenman's selectivity sequence I (Eisenman, 1962).

Table 3 presents the translocation energy barriers, taken as differences in energy between the first and the fourth ion position, for different values of $\epsilon_{background}$. These energies, especially for the larger $\epsilon_{background}$, are not inconsistent with values deduced from stochastic dynamic modeling of gramicidin conductance (Jakobsson and Chiu, 1987) or from computational chemical modeling of gramicidin's free energy profile (Roux and Karplus, 1993). Depending upon ion and method, translational barriers between 10 and 55 kJ/mol have been presented. The success that stochastic dynamics has had in correlating conductance data suggests that ionic movement through gramicidin is predominantly diffusive in nature, and indicates that the translational barriers are closer to 10 than 55 kJ/mol. In comparing different ions, we assume that translocational selectivity is determined by the conductance (Ω) of the aqueous pathway, and is thus dependent on both the height of activation energy barrier and internal friction. In the ohmic domain, the Nernst-Planck expression for Ω is (Levitt, 1986):

$$\Omega = \frac{CDAF^2}{N_o RT} \Big/ \int_0^L dz \exp\left[\frac{G(z)}{RT}\right] \qquad (3)$$

where C is the cationic concentration, D is its aqueous diffusion

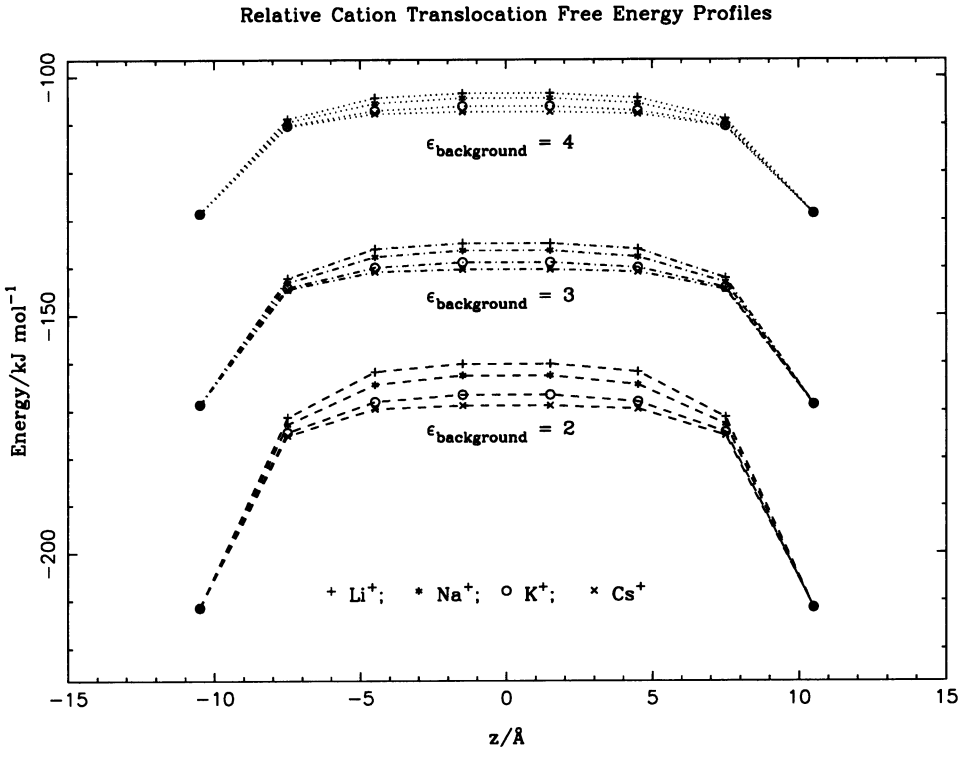

FIGURE 2 Relative free energy profiles for cation translocation as functions of $\epsilon_{background}$. For each set of free energy profiles, the energies have been shifted so that for a given value of $\epsilon_{background}$ energy is measured relative to energy at site 1 (or 8), $z \sim \pm 10.5$ Å. Thus, the absolute values of energy have no significance. As indicated in the text, the location of site N is both ion- and $\epsilon_{background}$-dependent.

TABLE 3 Translocational free energies (kJ/mol) and relative Selectivities as functions of $\epsilon_{background}$

	ϵ_{back} = 2		ϵ_{back} = 3		ϵ_{back} = 4		Exp.	
Ion	ΔG	Sel.	ΔG	Sel.	ΔG	Sel.	Sel.	(D_{ion}/D_{Na})*
Li^+	51.3	0.3	33.8	0.4	25.1	0.5		0.78
Na^+	48.9	1.0	32.3	1.0	24.1	1.0	1.0	1.00
K^+	44.8	6.4	29.9	3.6	22.4	2.7	2.1	1.50
Cs^+	42.6	15.0	28.3	6.1	21.2	3.9	6.3	1.55

*D_{ion}/D_{Na} is the ratio of ionic and Na^+ diffusion coefficients.

coefficient, A is the channel area, L is the channel length, F and N_0 are Faraday's and Avogadro's numbers, respectively. We define translocational Selectivity relative to Na^+ as Ω_{ion}/Ω_{Na}; for diffusion coefficients, we use the values for ions in bulk water and compare the computed selectivity ratios with experimental ionic translocation rates in gramicidin, normalized relative to Na^+ (Urban et al., 1980), $k_{t,X}/k_{t,Na}$. It is encouraging that despite the extreme simplicity of the model the experimental sequence is correctly reproduced. It should be noted that, although relative diffusibility accounts for much of the variation between Na^+ and K^+, this is clearly not the case for Cs^+. Numerical values are best accounted for with $\epsilon_{background}$ in the range of 3–4; with this choice calculated and experimental selectivities differ by less than a factor of two. The small differences between calculated selectivity and experimental translocation rate constant ratios is presumably due to the presence of specific local interactions that influence ionic permeability. Certainly the local interaction between gramicidin and Cs^+ or Na^+ differs sharply; in translocation, the former ion follows a trajectory that is nearly axial although the latter executes more of a spiral motion as it jumps from one carbonyl oxygen to the next (Skerra and Brickmann, 1987). Translocational selectivity in a gramicidin-like channel can be thus accounted for as a consequence of the balance between L-J and electrostatic interactions. The same favorable interactions that reduce image energy and allow ion passage produce an ion-specific permeability sequence. In the Eisenman theory of selectivity viewed as competition between ion interaction with bulk water and with the polar groups forming the ion-binding site (Eisenman, 1962), the $Cs^+ > K^+ > Na^+ > Li^+$ sequence (sequence I) occurs at low site field strength. In our image force model, with no specific site-ion (or ion-bulk water) interactions, a similar role to that of the field strength is played by the electrical permittivity of the transmembrane domain: lipid, peptide, and permeation pathway. It should be noted that in sequence I the ordering is the same as that of ionic mobilities in bulk water. Thus, our treatment of the effect of the surrounding dielectrics on translocation is, in essence, a "featureless channel" analog to theories of the influence of ionic size on mobility in water.

In addition to channel energetics, accounting for the influence of the short range potential demonstrates the possibility of significant site specific electrostriction associated with ion movement through a channel. Table 4 presents three measures of the effect, the ion-water separation ($z_{I\text{-}W}$), the

TABLE 4 Measures of site induced electrostriction (Å) as functions of $\epsilon_{background}$

Ion	Site	$\epsilon_{back} = 2$			$\epsilon_{back} = 4$		
		$Z_{I\text{-}W}$	$Z_{W1\text{-}W2}$	$Z_{W\text{-}W}$	$Z_{I\text{-}W}$	$Z_{W1\text{-}W2}$	$Z_{W\text{-}W}$
Li^+	1	2.36	3.06	3.17 ± 0.07	2.53	3.30	3.46 ± 0.08
	4	2.33	2.99	3.06 ± 0.06	2.48	3.20	3.28 ± 0.08
Na^+	1	2.62	3.06	3.16 ± 0.07	2.80	3.30	3.46 ± 0.08
	4	2.58	3.01	3.07 ± 0.06	2.75	3.21	3.29 ± 0.08
K^+	1	3.09	3.08	3.17 ± 0.06	3.29	3.32	3.47 ± 0.07
	4	3.05	3.03	3.08 ± 0.06	3.23	3.23	3.30 ± 0.07
Cs^+	1	3.44	3.08	3.17 ± 0.06	3.65	3.35	3.48 ± 0.06
	4	3.39	3.04	3.09 ± 0.05	3.59	3.25	3.32 ± 0.07

mean (channel-averaged) water-water separation ($z_{\langle W\text{-}W\rangle}$), and the separation between the water pairs neighboring the ion ($z_{W1\text{-}W2}$). Ion-water separation decreases only slightly as the ion moves into the channel; the effect is more pronounced for the larger ions. More dramatic effects are seen in the water-water separations. As the ion moves into the pore, there is a substantial drop in the separation of water pairs neighboring the ion; here the effect is more pronounced for the smaller ions. There is a striking decrease in the mean interwater separation as the ion moves into the channel; the effect is large and ion-independent. The qualitative picture is the same regardless of the value assigned to $\epsilon_{background}$; however, it is quantitatively greater for the larger $\epsilon_{background}$.

The various trends have simple interpretations in terms of the interaction between channel particles and with the surrounding bulk solvent. There are three interrelated effects, all leading to increased electrostriction as the ion moves deeper into the pore.

Attenuation of the ionic field is proportional to r^{-2}; thus, the effective number of strongly polarized neighbor channel waters increases as the ion moves further into the pore. For specificity, assume that this "polarization radius" extends for three waters (quite reasonable for $\epsilon_{background} = 2$–4 (Partenskii and Jordan, 1992b)). For an ion near the pore mouth, only three of the seven channel waters are close enough to interact strongly with it. There are six such waters for an ion near the pore center. Therefore, mean water dipole moments increase as the ion moves deeper into the pore; consequently, ion-water attraction is relatively stronger. This increased attraction leads to decreased ion-water separation; consequently, water-water distances diminish correspondingly.

A closely related argument focuses on the waters' polarization and direct water-water interaction. As the ion moves further into the channel, polarization of the water next to the ion increases, average water polarization increases, and individual polarizations attenuate less rapidly with increasing ion-water separation. Thus, there is greater water-water attraction, with correspondingly shorter interwater spacings. Because the polarization of the first neighbor water is also large, there is greater ion-water attraction leading to reduced ion-water distances.

A final argument concerns the influence image forces have on the ion-water interaction strength in the channel. As the ion moves away from the channel mouth, its electrical image moves further away from the channel-bulk water interface. Thus, image interaction with the water dipoles in the model pore is significantly reduced. The closest ion image is negatively charged repelling water dipoles to the right of the ion (see Fig. 1) and attracting ones to the left. The net effect is always to increases ion-water (and thus water-water) separation. The image-dipole interaction decreases quadratically with image-dipole separation. Because, for an ion on the left-hand side of the channel, the first image is located a distance $(r_I + 2(N - 1) \cdot r_W)$ from the channel-water interface, with N the position of the ion, it is clear that the ion image-channel water interaction drops very sharply as the ion moves away from the channel mouth. A similar argument can be made for the site dependence of changes in ion-water separation. An ion at the channel mouth is strongly attracted by its nearby image; the neighboring water is repelled by this image. For an ion near the center of the channel, the forces are weaker (the ion's images are further away) and nearly balanced because both ion and waters can interact equally well with the images in both aqueous regions. The differential effect argues for greater ion-water separation when the ion is near the mouth.

Because the short range 6–12 interactions are unaffected by the position of the ion, there is an abrupt decrease in the length of the water column as the ion moves into the channel, most conclusively demonstrated by the decrease in $z_{\langle W\text{-}W\rangle}$ and $z_{W1\text{-}W2}$. With $\epsilon = 2$, the ion-water chain length (corrected for differences in ionic size) decreases by ~0.65–0.75 Å as the ion moves from site 1 to site 4 (if $\epsilon = 4$, the drop is ~1.1–1.2 Å). The distance between the water pairs to either side of the ion (the first and second neighbor waters) drops noticeably as the ion moves from site 1 to site 4, by ~0.05–0.07 Å when $\epsilon = 2$ and ~0.1 Å when $\epsilon = 4$.

These significant changes are direct effects of long range ion-solvent and channel water-solvent interactions. This suggests that important qualitative correlations can be missed in MD calculations that do not properly take into consideration long range electrostatic influences. This would be especially serious in the interior of longer pores, where the distance between the ion and the bulk solvent exceeds the MD cutoff radius.

The sensitivity of ion-water and water-water separations to changes in $\epsilon_{background}$ only serves to illustrate a well known observation: parameter sets form a seamless whole (van Gunsteren and Mark, 1992). The 6–12 parameters we use were designed for MD simulations for which $\epsilon \equiv 1$. A totally internally consistent analysis would probably

demonstrate that changing $\epsilon_{background}$ has an impact on the values of the 6–12 parameters. A microscopic analysis of this effect might well be important for more reliable quantitative modeling of equilibrium channel properties.

CONCLUSIONS

The dipolar chain model, modified to account for ionic size, provides a reasonable quantitative rationalization for the relative permeabilities of alkali cations in a gramicidin-like channel. In gramicidin, with its quasi-periodic structure, channel selectivity can be accounted for without consideration of the channel's molecular structure. The results correspond to Eisenman's selectivity sequence I. In addition to accounting for translocational energetics, our analysis suggests that there is likely to be significant electrostriction in an ion-water chain as the ion moves away from the pore mouth and into the channel interior. Accounting for absolute permeation rates requires detailed molecular modeling.

This work has been supported by a grant from National Institutes of Health (GM-28643) and by a sabbatical grant from the Universidad Complutense de Madrid (M. Sancho).

REFERENCES

Chiu, S. W., J. A. Novotny, and E. Jakobsson. 1993. The nature of ion and water barrier crossings in a simulated ion channel. *Biophys. J.* 64:98–109.

Dilger, J. P., L. R. Fisher, and D. A. Haydon. 1982. A critical comparison of electrical and optical methods for bilayer thickness determination. *Chem. Phys. Lipids.* 30:159–176.

Duca, K. A., and P. C. Jordan. 1993. How polarizability and helix flexibility affect ion-water correlations in a gramicidinlike channel. *Biophys. J.* 64: 301*a*. (Abstr.)

Eisenman, G. 1962. Cation selective glass electrodes and their mode of operation. *Biophys. J.* 2S:259–323.

Fettiplace, R., D. M. Andrews, and D. A. Haydon. 1971. The thickness, composition and structure of some lipid bilayer and natural membranes. *J. Membr. Biol.* 5:277–296.

Franks, F. 1973. Water, A Comprehensive Treatise, Vol. 1. Plenum Publishing Co., New York.

Hasted, J. B. 1973. Liquid water: Dielectric properties. *In* Water, A Comprehensive Treatise, Vol. 1. F. Franks, editor. Plenum Publishing Co., New York.

Hille, B. 1992. Ionic Channels of Excitable Membranes, 2nd ed. Sinauer Associates, Sunderland, MA.

Hille, B., and W. Schwartz. 1978. Potassium channels as multi-ion single file pores. *J. Gen. Physiol.* 72:409–442.

Hirschfelder, J. O., C. F. Curtiss, and R. B. Bird. 1954. Molecular Theory of Gases and Liquids. John Wiley & Sons, Inc., New York.

Jakobsson, E., and S. W. Chiu. 1987. Stochastic theory of ion movement in channels with single ion occupancy. Application to sodium permeation of gramicidin channels. *Biophys. J.* 52:33–45.

Jayaram, B., B. Honig, K. Sharp, and R. Fine. 1989. Free energy calculations of ion hydration. An analysis of the Born model in terms of microscopic simulations. *J. Phys. Chem.* 93:4320–4327.

Jordan, P. C. 1984. The total electrostatic potential in a gramicidin channel. *J. Membr. Biol.* 78:91–102.

Jordan, P. C. 1990. Ion-water and ion-polypeptide correlations in a gramicidin-like channel. A molecular dynamics study. *Biophys. J.* 58:1133–1156.

Jordan, P. C., J. A. McCammon, R. J. Bacquet, and P. Tran. 1989. How electrolyte shielding influences the electrical potential in transmembrane ion channels. *Biophys. J.* 55:1041–1052.

Jorgensen, W. L., R. W. Impey, J. Chandrasekhar, J. D. Madura, and M. L. Klein. 1983. Comparison of simple potential functions for simulating liquid water. *J. Chem. Phys.* 79:926–935.

Koeppe II, R. E., and M. Kimura. 1984. Computer building of β-helical polypeptide models. *Biopolymers.* 23:23–38.

Kong, C. L. 1973. Combining rules for intermolecular potential parameters. II. Rules for the Lennard-Jones (12, 6) potential and Morse potential. *J. Chem. Phys.* 59:2424–2467.

Levitt, D. G. 1978. Electrostatic calculations for an ion channel. I. Energy and potential profiles and interaction between ions. *Biophys. J.* 22:202–219.

Levitt, D. G. 1984. Kinetics of movement in narrow channels. *Curr. Top. Membr. Transp.* 21:181–197.

Levitt, D. G 1986. Interpretation of biological ion channel flux data. Reaction-rate versus continuum theory. *Annu. Rev. Biophys. Biophys. Chem.* 15:29–57.

Lifson, S., and J. L. Jackson. 1962. On the self-diffusion of ions in a polyelectrolyte solution. *J. Chem. Phys.* 36:2410–2414.

Lin, S., and P. C. Jordan. 1989. Structures and energetics of monovalent ion-water microclusters. II. Thermal phenomena. *J. Chem. Phys.* 89:7492–7501.

Mackay, D. H. J., P. H. Berens, A. T. Hagler, and K. R. Wilson. 1984. Structure and dynamics of ion transport through gramicidin A. *Biophys. J.* 46:229–248.

Martinez, G., M. Sancho, and V. Fonseca. 1992. Study of the influence of the side chain dipoles on the conductance of ion channels formed by gramicidin analogues. *In* Charge and Field Effects in Biosystems, Vol. 3. M. J. Allen, S. F. Cleary, A. E. Sowers, and D. D. Shillady, editors. Birkhauser, Boston.

Miller, C. 1982. Bis-quaternary ammonium blockers as structural probes of the sarcoplasmic reticulum K channel. *J. Gen. Physiol.* 79:869–891.

Monoi, H. 1991. Effective pore radius of the gramicidin channel. Electrostatic energies of ions calculated by a three dielectric model. *Biophys. J.* 59:786–794.

Partenskii, M. B., M. Cai, and P. C. Jordan. 1991a. A dipolar chain model for the electrostatics of transmembrane ion channels. *Chem. Phys.* 153:125–131.

Partenskii, M. B., M. Cai, and P. C. Jordan. 1991b. The influence of pore-former charge distribution on the electrostatic properties of dipolar water chains in transmembrane ion channels. *Electrochem. Acta.* 36:1753–1756.

Partenskii, M., and P. C. Jordan. 1992a. Nonlinear dielectric behavior of water in transmembrane ion channels: ion energy barriers and the channel dielectric constant. *J. Phys. Chem.* 96:3906–3910.

Partenskii, M., and P. C. Jordan. 1992b. Theoretical perspectives on ion-channel electrostatics: continuum and microscopic approaches. *Q. Rev. Biophys.* 25:477–510.

Partenskii, M., and P. C. Jordan. 1993. Influence of a channel forming peptide on ion energy barriers in a continuous three-dielectric model for ion channels. *Biophys. J.* 64:301*a*. (Abstr.)

Press, W. H. 1992. Numerical Recipes in Fortran: The Art of Scientific Computing, 2nd ed. Cambridge University Press, Cambridge, U.K.

Roux, B., and M. Karplus. 1991a. Ion transport in a model gramicidin channel. Structure and thermodynamics. *Biophys. J.* 59:961–981.

Roux, B., and M. Karplus. 1991b. Ion transport in a gramicidin-like channel: dynamics and mobility. *J. Phys. Chem.* 95:4856–4868.

Roux, B., and M. Karplus. 1993. Ion transport in the gramicidin channel. Free energy of the solvated right-handed dimer in a model membrane. *J. Am. Chem. Soc.* 115:3250–3262.

Sancho, M., and G. Martinez. 1991. Electrostatic modeling of dipole-ion interactions in gramicidinlike channels. *Biophys. J.* 60:81–88.

Skerra, A., and J. Brickmann. 1987. Structure and dynamics of one-dimensional solutions in biological transmembrane channels. *Biophys. J.* 51:969–976.

Sung, S. S., and P. C. Jordan. 1986. Structures and energetics of monovalent ion-water microclusters. *J. Chem. Phys.* 85:4045–4051.

Tredgold, R. H., and P. N. Hole. 1976. Dielectric behavior of dry synthetic polypeptides. *Biochim. Biophys. Acta.* 443:137–142.

Urban, B. W., S. B. Hladky, and D. A. Haydon. 1980. Ion movements in gramicidin pores. An example of single-file transport. *Biochim. Biophys. Acta.* 602:331–354.

van Gunsteren, W. F., and A. E. Mark. 1992. On the interpretation of biochemical data by molecular dynamics computer simulation. *Eur. J. Biochem.* 204:947–961.

Wallace, B. A. 1990. Gramicidin channels and pores. *Annu. Rev. Biophys. Biophys. Chem.* 19:127–157.